Author's Accepted Manuscript

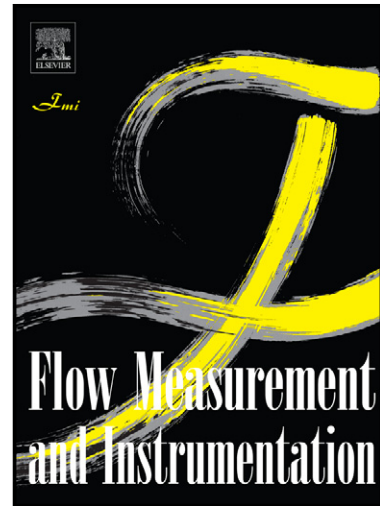*In Vitro* Assessment of Combined Doppler Ultrasound and CFD modeling in Arterial Blood Flow Quantification

Swandito Susanto, M. Skote, S. Chauhan

Cite this article as: Swandito Susanto, M. Skote, S. Chauhan, *In Vitro* Assessment of Combined Doppler Ultrasound and CFD modeling in Arterial Blood Flow Quantification, *Flow Measurement and Instrumentation*, http://dx.doi.org/10.1016/j.flowmeasinst.2013.07.013

In Vitro Assessment of Combined Doppler Ultrasound and CFD modeling in Arterial Blood Flow Quantification

Swandito [a,*], M. Skote [a,1,**], S. Chauhan [b]

[a]*School of Mechanical and Aerospace Engineering, Nanyang Technological University.*
50 Nanyang Avenue, Singapore 639798
[b]*School of Mechanical and Aerospace Engineering, Monash University.*
Building 72, Clayton campus, VIC 3800, Australia

Spatiotemporal quantification of the blood flow in the human vasculature has been greatly aided with the non-invasive proposition offered by Doppler ultrasound. However, relatively large deviation of the blood flow measurement from the actual value is expected, owing to a number of contributing factors. The research work expounded here attempts to ameliorate the accuracy of the blood flow output quantification by combining the Doppler measurement with the computational fluid dynamics modeling based on Navier-Stokes equation. *In vitro* assessment of the integrated approach was carried out with custom made phantom and probe positioning Mechatronic system. Analysis of the experimental results showed that, compared to the stand alone Doppler ultrasound measurement, the integrated model gives better accuracy in quantifying the volume flow rate.

Keywords: Computational Fluid Dynamics (CFD), Doppler ultrasound, Flow quantification, *In vitro* experimentation

1. Introduction

Accurate determination of *in situ* blood volumetric flow rate and pressure is of paramount importance for the prognosis and for the post-treatment assessment of many arterial diseases. Literature supports various analyses performed mainly through the empirical and constitutive relationship between the flow parameters and arterial properties [1], [2]. Non-invasive arterial blood flow quantification which previously possessed great challenge can now be performed with relative ease utilizing Doppler ultrasound techniques [3]. Hence, it is hardly a surprise

*Corresponding author
**Principal corresponding author
E-mail addresses: swandito1@e.ntu.edu.sg (Swandito), mskote@ntu.edu.sg (M.Skote), Sunita.Chauhan@monash.edu (S.Chauhan)
[1]Tel: +65- 67904271

that the number of Doppler applications in clinical practice has significantly increased during the last decade. Its utility has also been further extended and demonstrated for assessing the vasculature inside the human skull [3], [4]; overcoming the difficulty that arose from the anatomical location and the acoustic properties of the skull which in general hinder the applicability of the ultrasound. Doppler has also been used as an extension function to optical coherence tomography in measuring the blood flow [5].

Doppler Ultrasound Systems (DUS) use ultrasound waves as its sensing modality and generally have both continuous and pulsed wave in order to optimize each of its advantage [6]. They are also usually further enhanced with B-mode (Brightness-mode) where a linear array of transducers simultaneously scans a plane and display the scanning output as a two dimensional image on screen and other additional features which greatly improves its capability in extracting information pertinent to a particular flow at a specific location and time instance. However, despite all the advantages an ultrasound system can offer, its usability is also constrained by several limitations. Ultrasound requires a medium which has similar acoustic impedance to that of the ultrasound transducer's material in order to transfer the ultrasound beam effectively. In its due course, the beam experiences attenuation such as scattering, refraction, etc., thus limiting its depth of penetration or spatial resolution [7]-[9]. Careful preparation is required to fully maximize its functionality.

In addition to the above mentioned problems, all of the DUS systems also suffer from the problems incurred during the flow quantification such as measurement of the component of the velocity which is parallel to the axis of the Doppler transducer, determination of the angle between the axis of the flow and the transducer's axis, and last but not least the measurement of the cross-sectional area of the blood vessel [6], [10]. An error in measuring the angle between the transducer's axis and axis of the flow could be as large as 4 to 6% for every degree of error in its most accurate range of measurement angle (Figure 1) [9]. For example, if the error in determining the measurement angle is 2 degree, the error in flow volume quantification can be as large as 8 to 12% of the real flow volume. Most accurate range of measurement angle refers to the range of angle where the cosine (angle) changes less rapidly with change in the angle. This value of cos(angle) is important since it is one of the terms that constitute the formula of the Doppler flow volume quantification. For Doppler that also utilizes B-mode, the optimum measurement angle is about 60° [6]. Based on this, the error is expected to be larger when the measurement angle is not within the most accurate range of measurement. Similarly, an error in presuming the velocity vector could lead to significant over or underestimation of the volumetric blood flow. The error is also increased if, as in a typical volumetric calculation, the artery diameter is presumed to be constant, which is far from reality. Due to the pulsatile flow, the artery diameter changes with time since the arterial wall is a visco-elastic material. Even if the mean artery diameter is used during the calculation, for instance in the case of carotid artery, it could still lead to an estimated 0.4 to 3.6 % error in measurements [11]. And this does not include the fact that the artery is not a perfect circle and the presence of disease such as stenosis will further complicate the matter.

Several solutions to this problem have been presented. These include: the use of multiple transducers to give 2D or even 3D velocity vectors which is done in the effort to avoid making assumption on certain flow characteristics [12]; garnering multiple samples in a 2D plane instead of relying on uniform insonation in order to measure the shape of the instantaneous velocity profile [13]; development of an Attenuation Compensation method by producing two ultrasound beams with one beam used to calibrate the other [14]; and the development of the assumed velocity profile method which is the variation of Duplex

method, where the mean velocity is determined from the time-averaged maximum Doppler shift [15]. While these methods reduce the error, they require substantial amount of computational power and having multiple transducers create complications in system arrangement and calibration. Taking these issues in consideration, it appears that there is compelling reasons to re-assess the applicability of the Doppler ultrasound in the arterial blood flow quantification and to deduce an alternative or complementary approach to improve the flow measurement outcome.
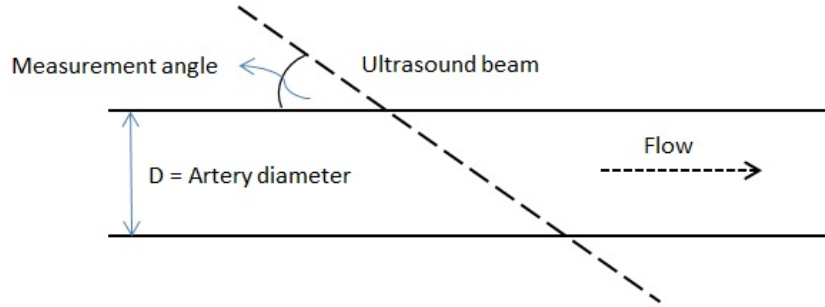

Figure 1 Doppler ultrasound beam measurement angle

Blood flow quantification through numerical modeling based on fluid dynamics equations are proposed in this paper to complement the measurements conducted by the DUS. Blood flow modeling itself has been studied extensively over time and plenty of researchers have attempted to develop them mostly using the Navier-Stokes (NS) equation and its simplified version [16]-[20]. During the course of the model development several assumptions were introduced mainly regarding the mechanics of the arterial wall. Each of the derived models validates and accounts for a certain paradigm and condition pertaining to a set of predefined nature. With the changes in the governing parameters, the output of the model may find it hard to reflect the real output. In quantifying the volumetric blood flow, for example inside the brain vasculature, for the purpose of knowing the state of, in this case brain perfusion, it is paramount that the estimation is highly accurate. In order to have a good model, it is necessary to have accurate representation or estimation of the governing parameters. However, it is also necessary to put some restraint to limit the complexity of the model to aid its efficiency and applicability in real-time situations. Unfortunately, as found in the precedential studies, even for the vigorously developed blood flow model, there is still discernible disparity between the measured blood flow and the theoretical/computational models [21]-[24]. This further impels for alternative integrated or complementary approach for blood flow modeling.

This paper elucidates the development of the combined Doppler ultrasound and CFD modeling for blood flow quantification. Findings obtained from earlier Doppler experiments by other researchers' show that there are weaknesses with regard to the Doppler ultrasound applicability and results. Likewise, the computational methodology has its own drawbacks, most notably the time consumption for obtaining realistic results. The combined approach presented here is intended to be an alternative way to improve the said weaknesses. The validation of the aforementioned approach involved an experimental set-up targeted to emulate the carotid artery on a simple level, as well as numerical simulations (CFD).

The research project elaborated here comprised two mains stages. The first stage was the verification of the efficacy of the Doppler ultrasound in measuring the volumetric blood flow in human body through an experimental set up. It was necessitated for the re-assessment of the Doppler ultrasound capability in performing arterial blood flow quantification. The second stage was the derivation of the flow model which was based on a custom built phantom for the validation.

The remainder of the paper is divided into a few sections as follows: Section-2 explains the *in vitro* Doppler experimental set-up and procedure, and the standalone Doppler measurement is expounded. Section-3 propounds the development of the CFD, while the integrated approach is presented in section-4, where the simulation output of the developed approach is also elaborated and discussed in detail. Finally, section-5 concludes the outcomes of this study along with suggestions for future work.

2. Doppler Ultrasound Experimentation

In this section, the experimental set-up along with the results of this study is presented. The accuracy of the Doppler technique depends mainly on the precise positioning of the ultrasound source with respect to the target blood vessel, measurement details of the vessel size, and the presence of interfering noises (e.g. artifact, bubbles) [6], [25]. When performing the experiments, these factors were minimized to optimize Doppler measurement. The following sub-sections give elaborate explanation with regard to the experimental fixture, testing procedure, testing results and discussions.

2.1. Experimental set-up

A mechanical arm was configured for positioning of the Doppler probe. The line diagram of the mechanical interface is given in figure 2. The Doppler probe was attached to the end-effector of the arm. The mechanical arm consisted of four degrees of freedom (DOF) for precise positioning of the ultrasound probe with respect to the predefined target. Commercially available linear guide [26] was utilized for better alignment and accuracy. The movement precision was expected to be within 0.1mm for translational axis and 0.1° for rotational axis. Available travel distance for each axis was ensured to have enough leverage for small distance transducer movement. Other features of the experimental set-up consisted of tissue mimicking phantom, blood mimicking fluid (BMF), BMF reservoir, pumping system which includes the tubing, Doppler ultrasound system, and the probe holder which was attached to the positioning system.

Agar whose acoustic properties are comparable to human tissue was selected as tissue mimicking phantom [27]. Table 1 shows *agar* properties compared to the International Electrochemical Commission (IEC) guideline. Doppler signal, when applied to blood flow, is collected from the scattered signal by the red cells suspension. The blood mimicking fluid (BMF) for Doppler ultrasound application should closely match the acoustic and mechanical properties of the blood. The BMF solution used here was made from the mixture of glycerol, sodium iodide and water. The composition of the mixture is, 37%, 16% and 47% respectively, based on the study by Majid *et al.* [28] who showed that the physical properties of this composition are able to mimic those of the blood. Table 2 gives the properties of the BMF.
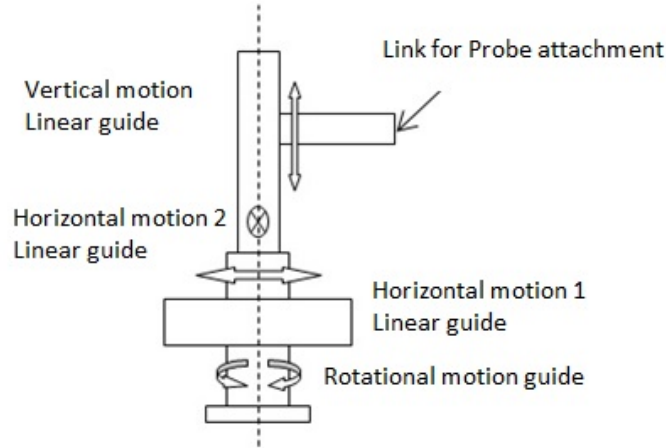
4

Figure 2 Schematic diagram of the mechanical arm

Table 1 Properties of the tissue mimicking material at room temperature (~295K) [6], [27]

Physical Quantity	IEC Standard	Agar
Density (kg m^{-3})	1040±100	1050±10
Velocity (m s^{-1})	1540±15	1540±10
Attenuation (dBcm^{-1} MHz^{-1})	0.5±0.05	0.5-0.85

A peristaltic pumping system (P100L-100, *Ravel Hiteks*) was used to pump the BMF through the phantom vessel [29]. By using the pump, the flow speed of the BMF can be varied (pump speed range from 0 to 99 RPM). The volumetric fluid flow is calculated from the reference formula given by the manufacturer (Eq. 1) with respect to the internal diameter (ID) of the silicone tubing that is used.

The ID of the silicone tubes employed were 2.7mm and 8mm respectively, which do not exactly correspond the internal diameter of the common carotid artery (CCA) and internal carotid artery (ICA) [30], which were attempted to be emulated, due to the difficulty of obtaining the suitable tube dimension. However, this did not pose a problem since the phantom was used to gauge the applicability and efficacy of the Doppler ultrasound, and slight differences in internal tube diameter were not expected to alter the outcomes. For each of the tubing, the pump roller was adjusted and the flow output calibrated manually by matching the actual flow output and the theoretical estimation:

$$Q_P = V_M F_T \qquad (1)$$

where, Q_P is the pump flow volume in ml/min, V_M is the motor's speed in RPM (Revolutions per Minute), and F_T is the tube flow rate in ml/rev.

Table 2 Properties of a standard BMF [6], [28]

Properties	IEC 1685 Draft Spec.	Human Blood @310K	BMF @~295K
Scattering Particle	-	Red Blood cell (RBC)	Glycerol
Particle size (μ m)	-	7	-
Hematocrit (% Vol.)	-	45	53
Density (kg m^{-3})	1050±40	1053	1244
Viscosity (mPa s)	4±0.4	3	4.31±0.03
Velocity (ms^{-1})	1570±30	1583	-
Attenuation (dB/cm MHz)	<0.1	0.15	-
Backscattering (dB)	Comparable to RBC	0	Comparable to RBC
Fluid properties	Newtonian	Non Newtonian	Newtonian

The Doppler ultrasound system used in this research was the Aloka Prosound SSD-3500SX Doppler system combined with the Aloka UST-5542 probe [31]. It comes with numerous delectable qualities that will enhance the sampling calculation of the velocity measurement such as quint frequency imaging, tissue harmonic echo, multi-beam processing capabilities, etc. The overview diagram of the experimental set up is shown in figure 3. As can be seen from the figure, the Doppler probe is attached to the mechanical arm's end-effector and subsequently positioned to interface with the phantom. The inset in figure 3 shows the attachment part where the probe is glued to the link which in turn is attached to the positioning jig. The probe is tangentially in contact with tissue phantom. To ensure constant contact, jelly is added to the surface of the phantom and the probe. Inside the phantom, BMF is circulated by the pump through the silicone tube.
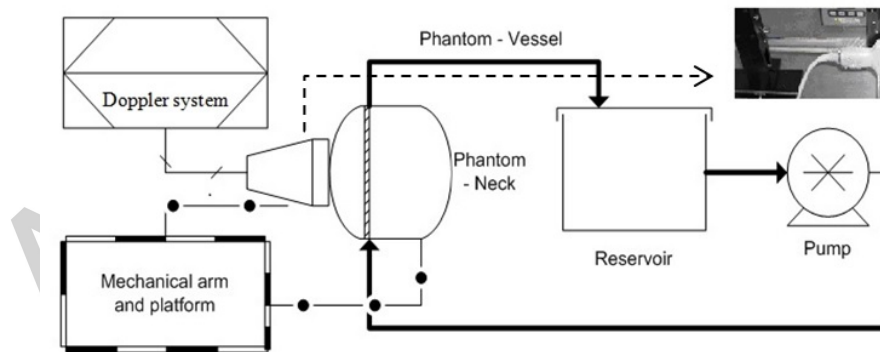
Figure 3. Overall schematic diagram of the experimental set-up.

2.2.Methodology

In order to calculate the volumetric fluid flow, the cross-sectional area of the flow vessel has to be determined. There are several methods to measure the cross sectional area and one of those methods uses the B-scan (otherwise also known as B-mode or 2D-mode) image. This method is considerably more effective than other methods, especially when the resolution of

the system is high and the positioning of the probe with respect to the blood vessel is known. Using the same imaging technique it is possible to see the vessel from different planar views, which help in determination of the vessel diameter. By placing the probe orthogonal to the vessel, the cross-sectional area can be determined. The probe was rotated by small angles to obtain the smallest diameter. It is imperative that the value of the diameter is captured as accurately as possible since a small deviation from the actual diameter will have significant effect on the volumetric blood flow due to the quadratic function of vessel diameter in the calculation of the total vessel area.

The area of the blood vessel was considered to be a perfect circle. However, this is not the case in an actual blood vessel. The circumference of the circle is not smooth and the diameter is changing periodically due to dynamics changes in blood pressure. In fact, it has been found that the variation in the common carotid artery is up to 6.7% based on a study by Beach *et al.* [32]. Other sources of errors can be ascribed to the limitation of the ultrasound axial resolution and uniformity of the ultrasound insonation. The angle of the ultrasound beam with respect to the blood vessel axis was determined by aligning a dedicated cursor on the B-scan image with the vessel axis. It was found that the optimum angle is about 60° where a good compromise between the B-scan and Doppler scan can be achieved. Accurate aligning poses a problem, especially since the flow is generally not totally parallel to the vessel axis and alignment of the probe with respect to the jig was not perfect. Furthermore, note that at 60° angle, the measurement error can be high considering that the cosine varies rapidly with the changes in the angle around 60°. The pump utilizes two rollers to achieve pressure gradient at the two sides of the tubes in order to make the fluid flow from one point to another. Simulating the pulsatile flow is understandably more difficult than the steady flow. The flow waveform is produced by using the pump through its flow cycle. It is theoretically possible to emulate the systole and diastole flow. However, in present experiment a constant flow rate within an emulated cardiac cycle is used.

In some of the Doppler images obtained from the experiments, reflected pressure waveforms could be found at the distal end of the tube due to the change in the impedance (see figure 4). The change in impedance created bipolar BMF flow, which is represented by two different color codes in figure 4, due to the discordance between the Doppler waveform and the flow waveform. Similar observations were reported from a study by Hoskins [33]. Furthermore, it is observed in figure 4 that flow outside of the tube boundaries (white horizontal lines) appears to exist. It is believed that these artefacts were caused by the noise signal associated with the high Doppler gain used [6] and possibly also due to the movement of the tube inside the agar. These problems were reduced if not eliminated in the following experiments by addressing the source problem (the gain used) and by introducing better holding mechanism for the tissue mimicking material and the BMF tube.

Due to the changing positions of the tubes and the roller adjustment, the output from the pump was expected to be slightly different from the theoretical calculation. In order to compare the theoretical output and the actual output from the pump, a number of tests were performed. Inaccuracy was observed which can be attributed to the measurement errors during the flow output calculation and the precision of the pumping timing. Nevertheless, the percentage of the error was less than 5% for almost all of the tests and this error seemed to be less when the flow velocity of the input was higher. Hence, it could be safely assumed that the actual output matches the theoretical output and therefore the theoretical calculation could be used for subsequent calculation where the nominal volumetric flow output was required.
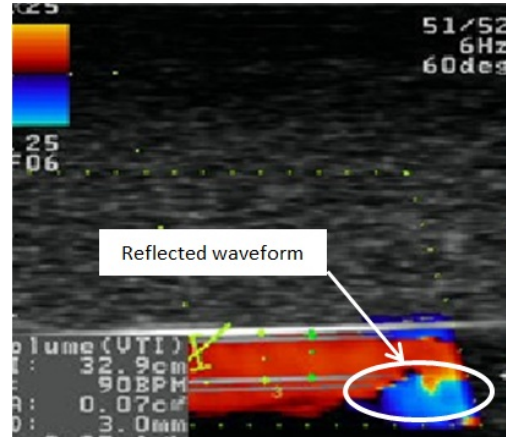
Figure 4 A Doppler flow image showing the reflected flow waveform

2.3.Accuracy of the Test

Flow in circular uniform tube is considered to be laminar when the Reynolds number (Re) is below a threshold which is commonly called the critical Re (Re_{crit}). For uniform tube the Re_{crit} is between 2000 – 2500 [34]. Using Eq. 2, it was theoretically verified that the BMF flow inside both tubes was generally laminar.

$$Re = \bar{v}D \Big/ \upsilon \qquad (2)$$

where, $\bar{v}$ is the average flow velocity, D is the diameter of the vessel and υ is the kinematics viscosity of the fluid.

The velocity profile of the flow changes over the tube length. Any upstream disturbances should have dissipated after certain length from the inlet and the flow is to be considered fully developed. The required entrance length for the flow development in this study can be calculated by using: $X = 0.03D(Re)$, where X is the required inlet length. This is the available formula to calculate the entrance length in circular tube for laminar flow [34]. From the computation, it was found that the actual tube length between the pump (inlet) and the Doppler measurement point is much longer than the required distance (more than three times) and thus it was inferred that the entrance effect in the tube flow has been nullified. However, unsteady flow could be seen qualitatively during the tests. This unsteady flow contributed to the inaccuracy in the velocity flow measurement due to the non-uniformity of the flow profile. One of the possible reasons for this was that even though the length is sufficiently long, the path was not totally straight, especially when the fluid was moving (there was no force applied to hold the tube in fixed position) and hence the unsteady flow observed during the experiment. This change in dimension which causes unsteady flow is well documented in many cases such as the one reported by Evans *et al.* [6] and Eriksen [11]. The flexibility of the silicone tube may be responsible for this as well. The extent of the unsteady flow's effect on volumetric flow calculation is difficult to estimate, apart from a few developed models in particular conditions [16-18].

In order to reduce the error due to the inaccuracy in determining the relative position of the probe and the target, a sensory system might be a viable solution. The sensory system needs

to be able to give a good measurement of the position and orientation of the target blood vessel. However, even though the position reference is accurate, the flow waveform does not really conform to the axis of the flow vessel. Hence, aside from having sensory plus automated system, model estimations of the flow waveform is needed for accurate estimation of correction angle and beam steering. Based on the conclusion inferred from previous tests, the tube is manually clamped and the position of the probe with respect to the predefined target is measured more vigorously in order to improve the results. Error in the volumetric flow output measurement is subsequently estimated at different motor speeds for different correction angles. This is done in order to verify the severity of the effect of the angle measurement inaccuracy toward the flow calculation. From the results, useful information could also be extracted for flow analysis.

To find out the relative position of the probe and the target, kinematics modeling was employed. Kinematics modeling of a manipulator structure is a way to describe a manipulator position with respect to a fixed Cartesian frame without concerning itself with the force and the moments that cause the motion [35]. The formulation of the kinematics model can be divided into two parts which are *forward kinematics* and *inverse kinematics*. The former is used to determine a general and systemic way to describe the motion of the end-effector as a function of the joint motion. Meanwhile, the latter concerns the transformation of the desired motion prescribed to the end-effector in the workspace into the corresponding joint motion [35]. The coordinate system was derived using modified Denavit-Hartenberg (D-H) method developed by Khalil *et al.* [36]. D-H is a standard robot kinematics model due to its value in physical interpretation, strict definition and applicability in multiplicative structure. On the other hand, the modified D-H refers to a D-H method with slight alteration in its derivation in order to eliminate the weakness of the original D-H method. For some positions in the joint space, due to the redundancy of the degree of freedom, more than one solution could be obtained. In order to have a unique solution, two scenarios were generated, one with moving rotational axis and one without moving rotational axis.

2.4. Results and Discussions

Figure 5 shows the measurement error for different sets of conditions. Each point in the polynomial fitting represents the average value of three experiment set of the same parameters. From the graph it can be seen that the flow measurement error (ε) increases exponentially in both direction deviating from the correct measurement angle (α). This finding conforms to the output produced by similar studies elaborated by Evans et al [6]. Fortunately, ε is relatively small (<5%) as long as the error in α is less than ~3°. In addition, it is beneficial to have smaller α (less than 60°) in order to minimize the ε caused by the error in α. However, the B-scan image requires the probe to be orthogonal to the target. Therefore, a compromise is needed and 60° measurement angle is considered to be optimum.

Triangulation was used to find the distance between the probe and the target in which two reference points are determined and the distance for the third point is found from the correlation of the known distance of the other two points and the third point. This was done in order to improve the measurement accuracy. It was determined that there are three sources for inaccurate measurement of the flow, namely probe placement within the holder, tissue mimicking phantom placement and vessel placement within the tissue mimicking phantom. Each of these three factors contributed 0 to 2° (absolute value) error in position measurement.

9

The inference came after a series of tests. In each set of tests (each set has 25 measurement sample), one parameter was measured (e.g. the probe placement). The manual measurement was done to a previously known distance of the measured object. The value of the manual measurement is then compared to the known value and the error was established. From the tests, it was found that the relative error is $<2°$ with majority is less than $1°$. The cumulative error, assuming the extreme case where all the maximum error from each possible error is added, can be as large as $\pm6°$ which in turn will give extremely high error in the volume flow calculation since the flow calculation depends on the cosine of the angle between probe beam and the flow vector. The relation between flow volume, velocity and the angle is described by [6]:

$$\overline{Q} = \frac{1}{T}\int_{t=0}^{T} A(t)\overline{v}(t)dt \qquad (3)$$

$$\overline{v}(t) = \frac{\overline{f}_d(t)c}{2f_t\cos\theta} \qquad (4)$$

where, $\overline{Q}$ is the average flow volume, $A(t)$ is the cross-sectional area of the vessel (which is taken as a constant), $\overline{v}(t)$ is the spatial mean velocity of the flow within the vessel, T is the total time period, $\overline{f}_d(t)$ is the instantaneous Doppler shift, f_t is the transmitted zero-crossing frequency, θ is the angle between the ultrasound beam and the vessel axis, and c is the velocity of ultrasound in the medium.
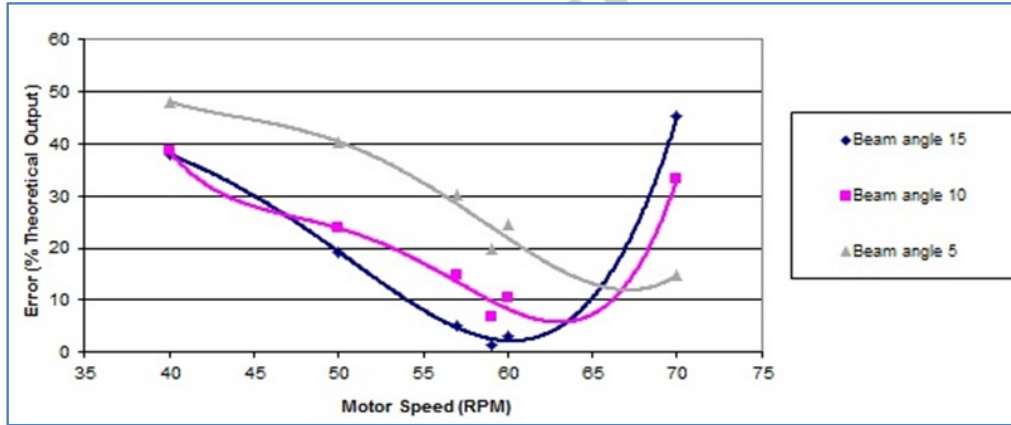

Figure 5 Measurement errors for different flow velocities with solid lines represent the polynomial curve fitting

It is perceived that the occurrence of the 'extreme' error (e.g. $\pm6°$) is small. To predict the most-likely-to-occur error, Gaussian distribution was employed, which may be formulated as [37]:

$$f_x(x) = \frac{1}{\sqrt{2\pi}\sigma}e^{\frac{-(x-\mu)^2}{2\sigma^2}} \qquad -\infty < x < \infty \qquad (5)$$

$$z = \frac{\chi - \mu}{\sigma} \qquad (6)$$

where, $f_x(x)$ is the central limit theorem probability density function, χ is the sample point, μ is the mean, σ is the standard deviation. For 95% confidence interval, $-1.96 < z < 1.96$.

10

For this experiment, the standard deviation is estimated to be $\sigma = 2$ in order for the calculation to remain truthful to the actual data while avoiding prediction which is overly conservative. This estimation can be further improved by taking more samples. However, in our case the samples taken are sufficient (n=25) to be the representative of the population. Using the calculation elaborated above with beam angle of 15°, a range of error in α was determined. Subsequently, the corresponding ε with respect to a range of α for different motor speeds were calculated and plotted in figure 6. From figure 6, it can be inferred that the flow output error will likely be under 12%. The $\sigma = 2$ used is considered large if automatic positioning system is employed since such mechatronics systems yield even better accuracy. It has to be noted that during the test some of the probe movement and measurement of the relative position are done/obtained manually and thus contributed to the measurement inaccuracy. The resulting measurement error can be reduced (substantially) if some automated (and sensory) system is used since accuracy in sub-mm is highly probable for an automated system [38]. Hence, it is expected that the result can be further refined.
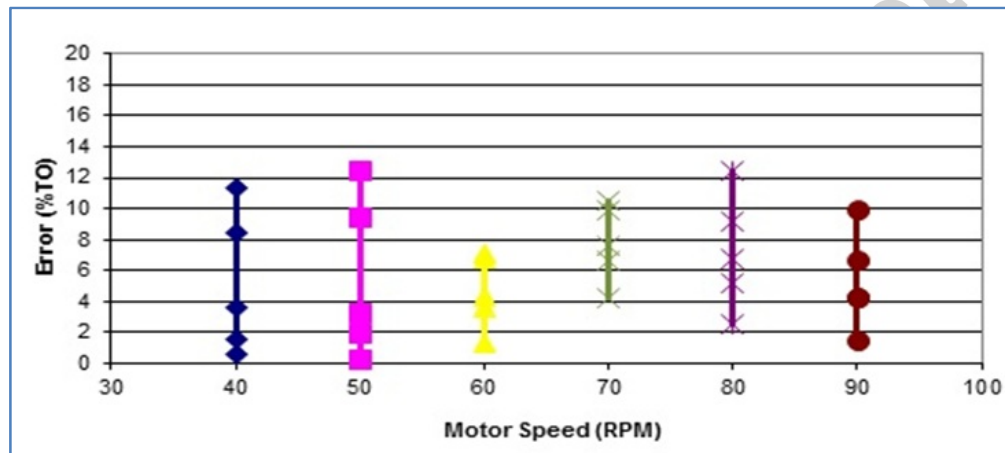

Figure 6 Errors interval for different pump's motor speeds and flow velocities

3. Blood Flow Modeling

The inputs from the ultrasound sensor complements the flow model developed either as an input parameter or a feedback parameter to fine tune the model. Following is the elucidation of the flow model development.

3.1. *Computational Fluid Dynamics*

Blood flow modelling has been studied in details for many years [16]-[24]. Various modelling parameters either stand alone or in combination with each other are presented in numerous publications. Most of them are intended to be used in specific part of the vasculature under certain conditions or assumptions. It is undeniably difficult to have a model that can cater for a wide range of predefined conditions. Even so, some researchers have tried to find a general model that can be used as a representative for a good range of vasculature variation, although slight modification is still needed. Arguably, it is close to impossible to find a universal model that can account for the variation of multitude parameters in a complex system of human physiology within the limit of the online calculation efficiency that is normally required.

11

The model developed by the authors was required to be able to give flow rates and possibly pressures in various discrete locations of the blood vessels. For the modelling, the CFD software, *Ansys-Fluent,* was utilized [39]. *Ansys-Fluent* was chosen because of its broad physical modeling capabilities. The integration of the *ANSYS-Fluent* into *ANSYS Workbench* provides superior platform with bi-directional connections to all major CAD systems and its flexibility to implement extensive customization based on user-defined functions.

There are a number of simulation stages in the process. The first was the modelling of the tube to be simulated. The modelling of the geometry was done in both *ANSYS Design Modeler* and by utilizing other CAD software after which the model was imported into the *ANSYS Design Modeler*. In this case *Pro/E* CAD software [40] was utilized because compared to the *ANSYS Design Modeler*, *Pro/E* is more versatile in creating complex shape and has many enhanced features that are superior compared to other CAD software such as its ability to model complex shape with relative ease. Once the model was generated in the *Pro/E*, it was then imported to the *ANSYS Design Modeler*. It should be noted that since the two of them are different modeling software, some incongruity may appear afterwards due to the import. For example, the overlapping portion of the model which may not be a problem in *Pro/E* may become the cause of inaccuracy in the *ANSYS*. Caution has to be taken in developing the model to take into account for these differences.

The next stage was the meshing of the model (figure 7). Unstructured mesh was generated for the model. Computer controlled parameters were used, for example, to determine the size of the mesh near the wall. Different grid sizes were applied in order to eliminate incorrect outcome. The third stage was to specify the relevant parameters and applicable user-defined function into the system before the simulation can be carried out. In this stage, parameters such as the type of the flow and boundary conditions, were varied for the purpose of analyzing the effect of each set of inputs on the simulation output. It is important that several assumptions with regard to the flow are properly defined before specifying these parameters as it has enormous effect on the outcome of the simulation [24]. For example, in all of the simulations, the tube wall was assumed to be impermeable. Hence the conservation of the mass was valid. The fourth and the last stage was analysing the simulation result. In this stage, the velocity profile of the BMF flow, pressure, *etc.* at various points could be visualized and plotted. Different parameters were examined for the purpose of the analysis which is further expounded in the next section.
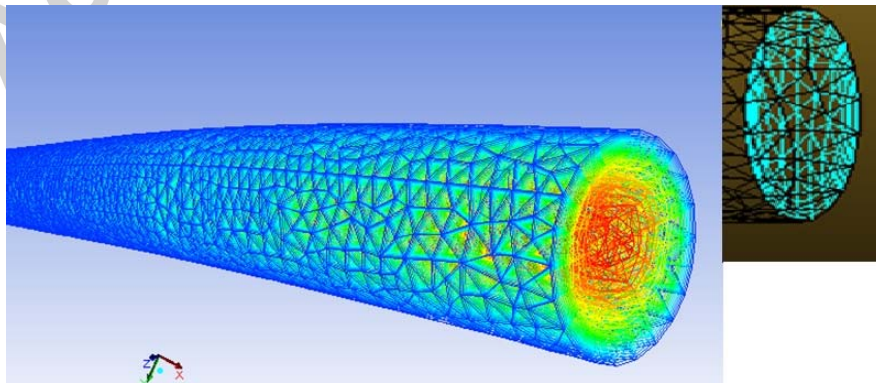

Figure 7 *Ansys Fluent* modeling – mesh. Each color represents different velocity with blue showing the lowest velocity while red showing the highest velocity

3.2.   Simulation Results

For the computer simulation, HP Workstation Z400 CPU (3.47GHz) 16 GB RAM was utilized. Processing time is in average less than one minute per set of simulation data. The short time might be attributed to the relatively good computing power and simple flow model simulated. Basic sensitivity analysis was performed by changing one parameters of the study at a time. For example, the flow velocity was increased slightly while the values of the other parameters remain the same. Aside from this, the size of the mesh was also varied, as indicated earlier, to remove uncertainties associated with inadequate mesh size. Arguably, this is one of the simplest sensitivity analyses possible. However, the simulation is very simple, and furthermore, its result could be directly correlated with the experimental outcome. Hence, it was presumed that this basic sensitivity analysis was adequate.

The simulated model generated different flow profiles for a slight change in the parameters such as model dimension, shape, the dynamics of the flow, governing equations, physiological parameters. It was well expected that multitude of these parameters contribute toward the model output for specified tube properties. Figure 8a shows the typical flow velocity profile generated at a partial arterial outlet. From the figure it can be seen that different flow velocity, as represented by different colour codes, are generated at different points across the cross-sectional area of the tube creating a parabolic shape with the highest velocity is at the axis of the flow. In order to give a clearer representation of the said velocity flow profile, a 2D flow profile taken from the centre of the 3D profile in figure 8a (line A-A) is re-illustrated by Figure 8b. In the diagram shown by figure 8b, the horizontal axis denotes the (radial) position and the vertical axis shows the corresponding velocity.
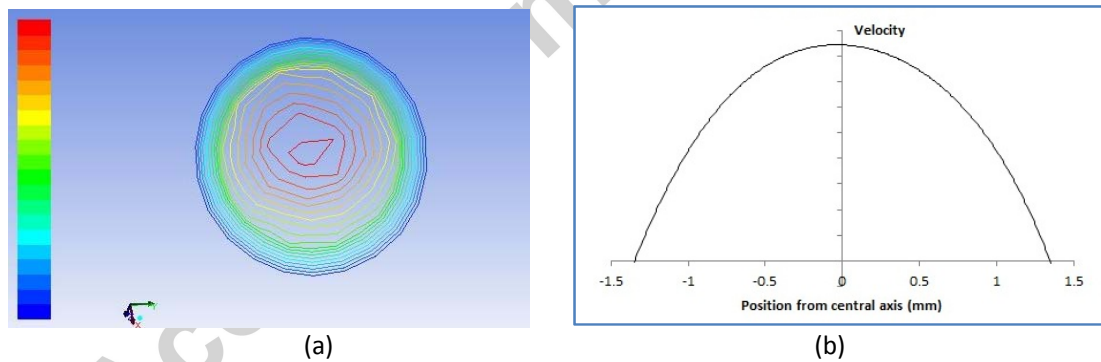

(a)   (b)

Figure 8 *Ansys Fluent* flow velocity profile. (a) Flow velocity profile at a partial outlet, blue color represents the lowest velocity while the red color represents the highest velocity. (b) Illustrative diagram of the 2D flow velocity profile taken from line A-A

4. Integrated Doppler and CFD Flow Model

Doppler measurement of the BMF flow velocity was used as a boundary condition at the predefined cross-sectional area in the CFD calculation. The point of measurement in the cross-sectional area is required to be estimated in order to establish the correlation between the Doppler sample and the flow profile, which in turn assists in improvement of the flow measurement accuracy. A set of different motor speeds input from the pump were defined for obtaining different flow input velocities. Using the input velocities, flow profiles for each

13

input velocity was generated by the CFD model and subsequently analyzed. From the analyses, the discrete point of measurement along the circular cross sectional area of the tube can be estimated by matching the Doppler flow at that point with the flow profile generated by the CFD.

Figures 9 and 10 show the placement of the measurement point along the tube circular cross-sectional area estimated from the CFD output based on Doppler samples. The samples were chosen in random manner. During the experiment, the insonation area might not be known exactly. Hence, correlation between the Doppler measurement points and CFD flow profile was deemed to be necessary to improve the accuracy of the quantification. In determining the location of the measurement point, an interval (of 0.05 mm) was used (e.g. a point located at 0.88 mm is said to be within 0.85 to 0.9 mm interval from the central axis). From the results shown in figure 9, the correlated measurement points were found to be in between 0.85 to 1.05 mm from the central axis of the tube. The shaded area in figure 10 shows the interval's relative position in the illustrated tube cross-sectional area. Using this result, it was assumed that all of the Doppler flow velocity measurement point was obtained from within this area. Using 0.85 and 1.05 as the lower and upper limit of the area, the mean 0.95 mm from the axis was taken as the areas where Doppler samples were taken and averaged.
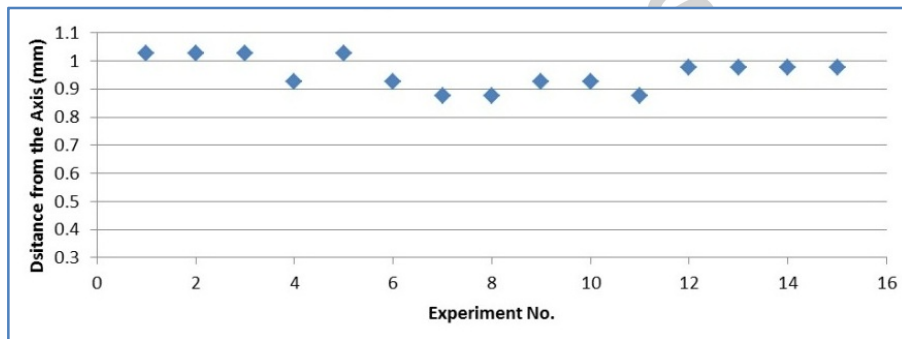

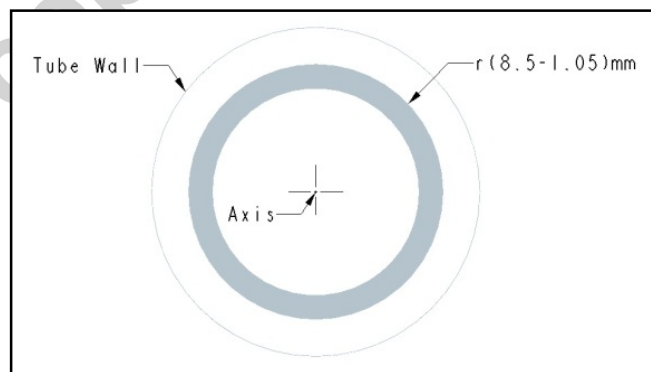**Figure 9** Estimated Doppler measurement point

Figure 10 Area of the point samples

Following the establishment of the Doppler measurement point, the BMF flow quantification obtained from the Doppler ultrasound measurement (as elaborated in section 2) was re-calculated. Among these original sets of flow velocity measurements obtained by the Doppler system, 15 sets were taken randomly. Each of these sets is associated with certain input parameters (i.e. motor speed, beam angle, correction angle) which were subsequently embedded in the CFD simulation. From the CFD simulation, a new flow profile was generated for each set. Based on the generated flow profile, volumetric flow output for each of the set was then calculated. In order to compare the output from stand-alone Doppler measurement and the combined model (Doppler plus CFD), the original flow volume obtained from Doppler and the flow volume calculation after the respective Doppler measurement had been embedded into the CFD model were subsequently analyzed.

Figure 11 shows the change in the flow quantification error from the stand alone Doppler measurements compared to the combined Doppler and CFD approach for different test sets. Clearly, the error percentage of the simulated flow output with respect to the theoretical flow output was improved for majority of the cases. Meanwhile, some experimental results did not experience any changes in the accuracy and a few suffer from worsening accuracy. The reason for the latter group could be attributed to the high accuracy obtained previously from the Doppler ultrasound measurement. When such accuracy has been obtained from the Doppler, the CFD appears to have limited ability to ameliorating it further. Hence, no changes in the error percentage and in one or two cases resulted in worse errors. However, it is noted that the improvement obtained far outweigh the undesirable output and even for the worsening errors, they are still within the error range shown in figure 7. It is thus inferred that the combined Doppler and CFD approach is able to give better accuracy than standalone Doppler measurement. The integrated approach is relatively simple to implement and within reasonable resource requirements of computing power and time consumption.

It could be observed that the flow simulated and validated in this study is very simple; the flow model used was laminar and there was no vigorous modeling of the tube or tissue mimicking fluid where, for example, the presence of viscoelasticity which will affect the output of the simulation. In addition, the geometry used is far from accurately emulating the arterial network of the human body. Nevertheless, the results shown here are encouraging and provide the foundation required for further and more complex studies.
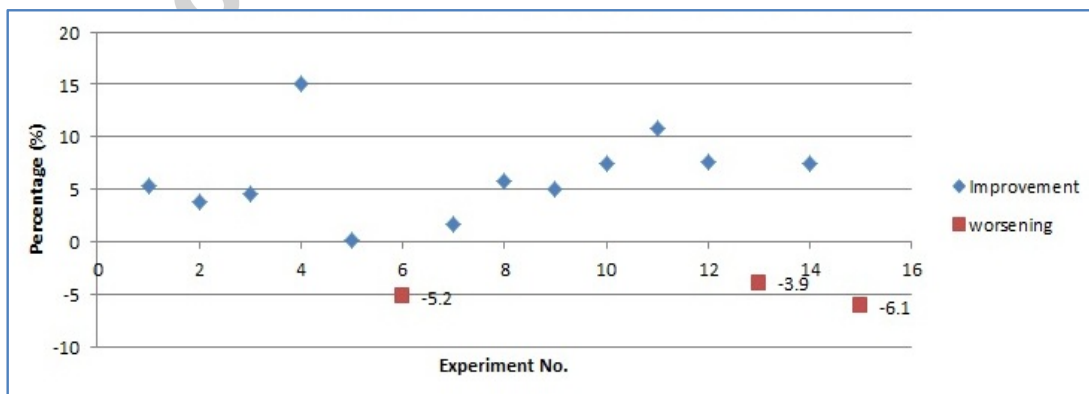

Figure 11 Change in the flow quantification error

5. Conclusions

The Doppler ultrasound experiment shows compelling result for the given application. From the experimental outcome, it was shown that the Doppler flow quantification errors were likely to be less than 12%. It is also concluded that the result can be further refined by employing automatic positioning system since automated system could be achieve higher accuracy as compared to the manual positioning which was done during the experiment. However, the achieved outcome was partly due to the meticulous way of determining the measurement angle and the relatively well-known phantom position. This will be much harder to achieve in real human application. It is possible to achieve better accuracy in moving the probe using the automatic system; however this is not the case in estimating the location of the artery. Thus, error due to the error in measurement angle could be very large and this is also backed by the study of Evans et al [6].

In order to further improve the output obtained from the Doppler measurement, a complementary approach based on CFD flow modeling was developed. The CFD model re-estimates the BMF flow output based on the input from the Doppler flow measurement. With this combined approach, even with the relatively accurate Doppler measurement, the CFD was shown to be able to yield improvement for the majority of cases except for those with exceptional accuracy. Even for the few cases with worsening error, the new error does not exceed the threshold (maximum error in the original error) and collectively the accuracy has gone up by about 4%. Admittedly, the flow simulated and validated in this study is very simple, for real human artery there are still much to be done, and, vigorous modeling is needed to accurately mimic the arterial blood flow with all its physiological properties. However, even with the most rigorous modeling, some discrepancy is still expected and each model gives accurate output mostly under specific condition [17-23]. The complexity of the model is also an issue since a more complex model requires higher computational power and time. With the combined model presented here, the weaknesses of each modality when is applied alone can be reduced.

The study presented in this paper is the first among a series of studies where the combinatory approach in quantifying the blood flow volume is studied. The validation of the approach elucidated in this paper is done after a relatively simple fluid flow case with limited parameters accounted for. However, albeit only a basic model, the result was encouraging and provided the foundation required for further and more complex studies. Following this, a more realistic emulation of actual blood flow will be established for which the proposed combinatory approach will be further improved and subsequently validated.

Acknowledgement

References

[1] Beulen BW, Bijnens N, Koutsouridis GK, Brands PJ, Rutten MC, van De Vosse FN. Toward Noninvasive blood pressure assessment in arteries by using ultrasound. Ultrasound Med Biol. 2011 May; 37(5):788-97.

[2] Leguy CA, Bosboom EM, Hoeks AP, van de Vosse FN. Assessment of blood volume flow in slightly curved arteries from a single velocity profile. J Biomech. 2009 Aug; 42(11): 1664-72.

[3] Willie CK., Colino FL, Bailey DM, Tzeng YC, Binsted G, Jones LW, *et al*. Utility of transcranial Doppler ultrasound for the integrative assessment of cerebrovascular function. J Neurosci Methods. 2011 Mar;196(2): 221-37.

[4] Thomas LC, Rivett DA, Bolton PS. Validity of Doppler velocimeter in examination of vertebral artery blood flow and its use in pre-manipulative screening of the neck. Man Ther. 2009 Oct; 14(5):544-9.

[5] Edmund K, Daniel H, Siqian W, Maximiliano C, Julia W. Resonant Doppler imaging with common path OCT. Proc. SPIE 7372, Optical Coherence Tomography and Coherence Techniques IV: 2009 July 13; Munich, Germany.

[6] Evans DH, McDicken WN. Doppler Ultrasound: Physics, Instrumentation and Signal Processing. 2nd Ed. England: John Wiley & Son; 2000.

[7] Liu GY, Burns PN. The attenuation compensated C-mode flowmeter: a new Doppler method for blood volume flow measurement. In: Schenider SC, Levy M, McAvoy BR (Eds). Proceedings of the 1997 IEEE Ultrasonics Symposium; 1997 Oct 5-8; Piscataway, US. Ont: Sunnibrook; 1997. p. 1285-9.

[8] Messer M, Aidun CK. Main effects on the accuracy of Pulsed-Ultrasound-Doppler-Velocimetry in the presence of rigid impermeable walls. Flow Measurement and Instrumentation. 2009 Apr; 20(2):85-94.

[9] Kremkau F. Doppler Error Angle due to Refraction. Ultrasound Med Biol. 1990; 16(5):523-4.

[10] Hill CR, Bamber JC, Haar GR. Physical Principle of Medical Ultrasonics. 2nd Ed. England: John Wiley & Sons; 2004.

[11] Eriksen M. Effect of pulsatile arterial diameter variations on blood flow estimated by Doppler ultrasound. Med Biol Eng Computing, 1992; 30(1):46-50.

[12] Kitabake A, Tanouchi J, Yoshida Y, Masuyama T, Uematsu K, Kamada T. Quantitative color flow imaging to measure two-dimensional distribution of blood flow velocity and the flow rate. Jap Circ J. 1990; 54:304-9.

[13] Deane CR, Markus HS. Colour velocity flow measurement: *in vitro* validation and application to human carotid arteries. Ultrasound Med Biol. 1997; 23:447-52.

[14] Gibson WGR, Cobbold RSC, Johnston KW. Principles and design feasibility of a Doppler ultrasound intravascular volumetric flowmeter. IEEE Trans Biomed Eng. 1994; 41:898-908.

[15] Li S, Hoskins PR, Anderson T, McDicken WN. Measurement of mean velocity during pulsatile flow using time-averaged maximum frequency of Doppler ultrasound waveforms. Ultrasound Med Biol. 1993; 19:105-13.

[16] Li JK, Cui T, Drzewiecki GM. A Nonlinear Model of the Arterial System Incorporating a Pressure Dependent Compliance. IEEE Trans Biomed Eng. 1990 Jul; 37(7):673-8.

[17] Nichols W, McDonald MF. Blood Flow in Arteries: Theoretic, Experimental and Clinical Principles. 3rd Ed. Lea & Febiger's; 1990.

[18] Johnson DA, Rose WC, Edwards JW, Naik U, Beris AN. Application of 1D blood flow models of the human arterial network to differential pressure predictions. J Biomech. 2011 Mar 15;44(5): 869-76.

[19] Johnson DA, Spaeth JR, Rose WC, Naik UP, Beris AN. An impedance model for blood flow in the human arterial system. Part I: model development and MATLAB implementation. J Biomech. 2011 July 11; 35(7):1304-16.

[20] Diourte B, Siche JP, Comparat V, Baquet JP, Mallion JM. Study of Arterial Blood Pressure by a Windkessel Type Model: Influence of Arterial Functional Properties. Comput Methods Programs Biomed. 1999 Jul; 60(1):11-22.

[21] Ottesen JT, Olufsen MS, Larsen JK. Applied Mathematical Model in Human Physiology. Monographs on Mathematical Modeling and Computation. Denmark; 2006.

[22] Alastruey J, Parker KH, Peiro J, Byrd SM, Sherwin SJ. Modelling the circle of Willis to assess the effects of anatomical variations and occlusions on cerebral flows. J Biomech. 2007; 40(8):1794-1805.

[23] Misra JC, Pal B. A Mathematical model for the study of the pulsatile blood flow of blood under an externally imposed body acceleration.' Mathematical and Computer Modeling. 1999 Jan; 29(1): 89-106.

[24] Raghu R, Taylor CA. Verification of a one-dimensional finite element method for modelling blood flow in the cardiovascular system incorporating a viscoelastic wall model'. Finite Elem Anal Design. 2011; 47(6): 586-92.

[25] Li W, van der Steen AF, Lancee CT, Cespedes I, Bom N. Blood flow imaging and volume flow quantification with intravascular ultrasound. Ultrasound Med Biol. 1998 Feb; 24(2):203-14.

[26] THK Co, Ltd. [internet]. Singapore: THK Global; c2011 [updated 2011; cited 2012]. Linear guide. Available from: http://www.thk.com/

[27] Burlew MM, Madsen EL, Zagzebski JA, Banjavic RA, Sum SW. A new ultrasound tissue-equivalent material. Radiology. 1980 Feb; 134(2):517-20.

[28] Majid YY, David WH, Tamie LP. A blood mimicking fluid for particle image velocimetry with silicone vasculars models. Experiments in Fluids. 2011; 50(3):769-74.

[29] Ravel Hiteks Pvt. Ltd. [internet]. India: Ravel Hiteks; c2008 [updated 2008; cited 2011]. Peristaltic Pump: RH-P100L-100. Available from: www.ravelhiteks.com

[30] Frederic M. Fundamentals of Anatomy and Physiology. 7th Ed. Pearson Benjamin Cummings; 2006.

[31] Hitachi Aloka Medical. Japan: Aloka Inc.; c2011 [updated 2011; cited 2011]. Doppler Ultrasound Prosound – 3500. Available from: http://www.aloka.com/products/view_system.asp?id=3

[32] Beach KW, Dunmire B, Overbeck JR, Waters D, Bileter M, Labs KH *et al*. Vector Doppler systems for arterial studies. Part 1: Theory. J Vasc Invest. 1996; 2(4):155-65.

[33] Hoskins PR. Peak Velocity Estimation in Arterial Stenosis Models using Color Vector Doppler. Ultrasound Med Biol. 1997; 23(6):889-97.

[34] William MD. Analysis of transport phenomena. Oxford; 2011.

[35] Schilling RJ. Fundamentals of Robotics: Analysis and Control. Singapore: Prentice-Hall; 1990.

[36] Khalil W, Kleinfinger JF. A New geometric notation for open and closed-loop robots. Proceedings of IEEE on robotics and automation; 1986; San Francisco: USA. p. 1174-9.

[37] Antonisamy B. Biostatistics: principles and practice. New Delhi: Tata McGraw Hill Education; 2010.

[38] Swandito S, Sunita C. A Hybrid Control Approach for Non-invasive Medical Robotic Systems. J Intell Robot Sys. 2010 Oct; 60(1):83-110.

[39] Ansys, Inc. [internet]. Global: Ansys; c2013 [updated 2013: cited 2012]. Ansys-Fluent. Available from: http://www.ansys.com

[40] PTC, Inc. Global: Parametric Technology Corporation; c2013 [updated 2013: cited 2012]. Pro/E – Creo elements. Available from: http://www.ptc.com

Swandito is a PhD student in Nanyang Technological University, Singapore. He received his B. Eng. and M. Eng. in mechanical engineering from Nanyang Technological University, Singapore, in 2004 and 2007, respectively. His research interests include biomechanics and medical robots design and control.

Assistant Professor Martin Skote joined the School of Mechanical & Aerospace Engineering, Nanyang Technological University, Singapore, in 2008. He received his Master and Ph.D. degrees from the Royal Institute of Technology (KTH) in Stockholm, Sweden. His research interests include Boundary layers, Atmospheric flow, and Turbulence control. His fundamental research on turbulence has been published in the Journal of Fluid Mechanics and Physics of Fluids. Prior to joining NTU, he worked for the Institute of High Performance Computing for three years, where he developed a numerical simulation tool for air pollution dispersion simulations in collaboration with the National Environment Agency, Singapore.

Associate Professor Sunita Chauhan obtained her PhD from Imperial College of Science, Technology and Medicine, University of London, United Kingdom, in 1999. She has been appointed Assistant Professor (1999-2005) and Associate Professor (2005-2012) at the School of Mechanical & Aerospace Engineering, Nanyang Technological University, Singapore. Her current research interests include Medical/surgical robotics, Computer Assisted/Integrated Surgery, Bio-mechatronics, Medical Instrumentation, Robotics, Mechatronics, Advanced Control, Sensors/Transducers, Ultrasound in Medicine (Diagnostic, Therapeutic, Surgical).

Highlights

- An improved method for quantifying blood flow in human vasculature is developed
- A combination of Doppler ultrasound and CFD modeling technique is utilized
- Assessment is done *in vitro* with custom made phantom and mechatronics system
- The integrated method yields better accuracy than stand-alone Doppler measurement